# Photoinduced Ultrafast Dynamics of $Ru(dcbpy)_2(NCS)_2$-Sensitized Nanocrystalline $TiO_2$ Films: The Influence of Sample Preparation and Experimental Conditions

**Jani Kallioinen,*,† Gábor Benkö,‡ Pasi Myllyperkiö,†,‡ Leonid Khriachtchev,§ Björn Skårman,# Reine Wallenberg,# Markus Tuomikoski,⊥ Jouko Korppi-Tommola,† Villy Sundström,‡ and Arkady P. Yartsev*,‡**

*Department of Chemistry, University of Jyväskylä, P.O. Box 35, FIN-40014 Jyväskylä, Finland, Department of Chemical Physics, Lund University, P.O. Box 124, SE-22100 Lund, Sweden, Laboratory of Physical Chemistry, University of Helsinki, P.O. Box 55, FIN-00014 Helsinki, Finland, Department of Materials Chemistry, Lund University, P.O. Box 124, SE-22100, Lund, Sweden, and VTT Electronics, P.O. Box 1100, FIN-90571 Oulu, Finland*

*Received: October 29, 2003; In Final Form: February 5, 2004*

In most of the previous ultrafast electron injection studies of $Ru(dcbpy)_2(NCS)_2$-sensitized nanocrystalline $TiO_2$ films, experimental conditions and sample preparation have been different from study to study and no studies of how the differences affect the observed dynamics have been reported. In the present paper, we have investigated the influence of such modifications. Pump photon density, environment of the sensitized film (solvent and air), and parameters of the film preparation (crystallinity and quality of the film) were varied in a systematic way and the obtained dynamics were compared to that of a well-defined reference sample: $Ru(dcbpy)_2(NCS)_2-TiO_2$ in acetonitrile. In some cases, the induced changes in the dynamics were uncorrelated to the electron injection process. High pump photon density (not in the linear response region) and exposure of the sensitized film to air altered the picosecond-time-scale kinetics considerably, and the changes were attributed mostly to degradation of the dye. In other cases, changes in the measured kinetics were related to the electron injection processes: reducing the firing temperature of the nanocrystalline film or making the film via electron beam evaporation (EBE) resulted in a decrease of the overall crystallinity of the film, and the electron injection slowed. In the sensitized EBE films, in addition to an increased contribution of triplet excited-state electron injection, a new electron transfer (ET) process with a time constant of 200 fs was observed.

## 1. Introduction

Dye-sensitized solar cells (DSSCs), where the photoactive electrode is prepared from RuN3-sensitized nanocrystalline titanium dioxide ($TiO_2$) thin films (RuN3 = $Ru(dcbpy)_2(NCS)_2$, where dcbpy = 2,2′-bipyridyl-4,4′-dicarboxylic acid), are capable of solar-energy-to-electricity conversion efficiencies of up to 10%.[1] The primary step in energy conversion is the absorption of a photon and the ensuing electron transfer (ET) from the excited state of RuN3 (RuN3*) into the conduction band of the $TiO_2$ nanoparticle (which is also called electron injection). The high energy-conversion efficiency[1] and stability[2,3] of the RuN3-sensitized $TiO_2$ cells has inspired an active study of the kinetic processes. The electron injection kinetics have been intensively studied, using transient absorption spectroscopy in the visible (vis), near-IR, and mid-IR regions.[4−16] The overall outcome of these studies has been important for understanding the function of the cell. Some of the results have not been free of controversy. To illustrate the similarities and differences of these studies, reported ET time constants and amplitudes are listed in Table 1, together with the RuN3−$TiO_2$ film environment and characteristic pump and probe wavelengths. In several studies, the fastest phase of electron injection is reported to be faster than the time resolution of the measurement and the time constant of the initial ET kinetics was resolved only very recently.[14] Thus, in a transient absorption study of Benkö et al.[14] the formation of the dye cation and the excited triplet state, as well as the decay of the singlet excited state were shown to be characterized by a time constant of 30 fs, which was concluded to reflect the rate of two parallel ultrafast processes: ET from the initially excited singlet state of RuN3 to the conduction band of $TiO_2$ and intersystem crossing (ISC). From the amplitude ratio of the processes, it was estimated that the rate constants of ET from the singlet excited state and ISC were $\sim^1/_{50}$ $fs^{-1}$ and $\sim^1/_{75}$ $fs^{-1}$, respectively. The role of the slower, picosecond-time-scale ET process has been a source of major controversy in the literature. In different studies, the reported rate of the slowest electron injection has varied by as much as a factor of 100 and the relative amplitude of the picosecond-time-scale ET has ranged between 0% and 71% (see Table 1).[4−16] In the studies where a significant contribution of the picosecond-time-scale ET processes were observed, the kinetics were nonexponential and were fitted with time constants ranging from ∼1 ps to ∼100 ps.[4,10,11,13−16] The nonexponential behavior of the ET kinetics becomes visible for accurately recorded signals. The picosecond phase of electron injection has been concluded to originate from the triplet excited state of RuN3.[14,15] The pronounced contribution of picosecond-time-scale ET that

* Authors to whom correspondence should be addressed. E-mail addresses: Arkady.Yartsev@chemphys.lu.se, jakallio@cc.jyu.fi.
† University of Jyväskylä.
‡ Department of Chemical Physics, Lund University.
§ University of Helsinki.
# Department of Materials Chemistry, Lund University.
⊥ VTT Electronics.

10.1021/jp037265v CCC: $27.50 
Published on Web 04/23/2004

**TABLE 1: Summary of Earlier Results on Electron Transfer (ET) Kinetics of RuN3-Sensitized $TiO_2$ Films**

| wavelength (nm) | | time constants and amplitudes[a] | | environment of RuN3−$TiO_2$ film | |
|---|---|---|---|---|---|
| pump | probe[b] | (fs) | (ps) | environment | reference |
| 605 | 750 | <150 (50%) | 1.2 (50%) | EC/PC[c] | Tachibana et al.[4] |
| 550 | 1100 | <25 | | UHV[d] | Hannappel et al.[5] |
| 400 | 4630 | <50 | | air | Ellingson et al.[8] |
| 400 | 4730 | 50 (>84%) | 1.7 (<16%) | air | Asbury et al.[9] |
| 520 | 760 | <100 (35%) | 1.3 (22%); 13 (43%) | EC/PC;[c] air | Durrant et al.[10] |
| 560 | | | | | |
| 600 | | | | | |
| 560 | 760 | <100 (29%) | 1.0 (25%); 13 (46%) | EC/PC[c] | Tachibana et al.[11] |
| 590 | 5400 | <350 | | DCM[e] | Heimer et al.[12] |
| 540 | 810 | <150 (44%) | 1.1 (20%); 12 (23%); 100 (13%)[f] | $N_2$ | Kallioinen et al.[13] |
| 530 | 860 | 28 (50%) | 1.0 (11%); 9.5 (12%); 50 (7%)[f] | acetonitrile | Benkö et al.[14] |
| 455 | | ≤20 (70%) | 1.8 (15%); 10 (3%); 50 (12%)[f] | | |
| 595 | 760 | <150 (30%) | 0.7 (25%); 17 (45%) | EC/PC[c] | Tachibana et al.[16] |

[a] Values given in parentheses represent the signal amplitudes. [b] If several wavelengths were used in the study, only one wavelength is listed, to characterize the wavelength region. [c] Mixture of ethylene carbonate and propylene carbonate (1:1). [d] Ultrahigh vacuum. [e] Dichloromethane. [f] The amplitudes of the components are not corrected, to eliminate the contribution of excited-state absorption.

has been demonstrated in these studies[4,10,11,13−16] is in sharp contrast to earlier studies, where the mid-IR region was used for probing. In these measurements, the reported ET kinetics were significantly faster and the slowest reported time constant was 1.7 ps.[8,9,12] Possible reasons for the discrepancy could be differences in measurement parameters (choice of probe wavelength and, thus, monitored species) and in sample preparation.[11,17] As a consequence of these differences, it becomes difficult to compare results from all these studies without knowing how the differences in measurement setups and sample preparation have influenced the kinetics.

In addition to dissimilar probe wavelengths, various excitation wavelengths have been used in earlier studies (see Table 1). The steady-state absorption spectrum of RuN3 on nanocrystalline $TiO_2$ film in acetonitrile has two main absorption bands in the visible region, with maxima at 400 and 539 nm, and a small shoulder at 656 nm in the red wing of the red-most band.[15] In most of the earlier studies, excitation was conducted close to the absorption band maxima of the RuN3 dye, i.e., close to 539 or 400 nm. In two studies, several wavelengths were used; Durrant et al.[10] studied the excitation wavelength dependence of the electron injection, using the wavelengths 520, 560, and 600 nm (all within the low-energy main absorption band), and Benkö et al.[14] used the excitation wavelengths of 455 nm (the contribution from both main absorption bands) and 530 nm (close to the maximum of the low-energy main absorption band). In the experiments of Durrant et al.,[10] similar ET kinetics were recorded for all excitation wavelengths; however, in the study of Benkö et al.,[14] a wavelength dependence of the ultrafast electron injection was observed. In that work, the electron injection rate was observed to increase when the excitation wavelength changed from 530 nm to 455 nm. This shows that the fastest component of electron injection is dependent on the initially populated electronic state: the higher the initially excited state, the faster the electron injection (this result suggests that, with excitation at 400 nm, faster ET kinetics could be expected than with excitation at ~600 nm, and this is actually what has been reported (see Table 1)). Whether this explains the variation of electron injection times supported by the data in Table 1 is not at all obvious, because many other parameters may have an impact on the ET kinetics.

In transient absorption measurements, pump and probe wavelengths, as well as excitation photon density, are important. To record the correct kinetics, a linear response of the signal as a function of pump intensity must be obtained. Earlier studies have reported pump photon densities that vary from $2 \times 10^{15}$ photons/cm$^2$ to $3 \times 10^{14}$ photons/cm$^2$,[4,8,9,11,13−16] and in the study by Heimer et al.,[12] a clearly higher pump photon density of $\sim 8 \times 10^{16}$ photons/cm$^2$ was used. In the present study, we will estimate the limit of the linear response region and determine what changes are imposed on the transient absorption signal due to high excitation photon densities.

So far, our discussion has focused on differences in the measured ET that may be related to the specifics of the transient absorption measurement; however, the sample itself is at least as important. Although a nanocrystalline $TiO_2$ film has been used as an electron acceptor and RuN3 dye has been used as an electron donor in all previous studies, there are several differences among the samples. First, the sensitized RuN3−$TiO_2$ films were kept in very different environments during the experiments—under vacuum, in the gas phase, and in various solvents (see Table 1). In some cases, very similar ET time constants were reported in different environments; however, on the other hand, there are also substantial differences from study to study. For instance, Durrant et al.[10] reported the same kinetics for ET in air and in ethylene carbonate/propylene carbonate (1:1) solution, and it was concluded that solvation dynamics did not have a significant effect on the injection kinetics. All kinetics were fitted with time constants ranging from <100 fs to ~13 ps. When measuring the RuN3−$TiO_2$ system in a nitrogen gas environment, Korppi-Tommola et al.[13] showed rather similar time constants to those measured by Durrant and co-workers,[10,11] with an exception that a new component with a time constant of 100 ps was also related to the ET kinetics. Picosecond-time-scale ET also has been observed in acetonitrile and the slow part of the kinetics ($\tau \geq 1$ ps) was nonexponential and could be fitted with time constants ranging from ~1 ps to ~60 ps.[14,15] On the other hand, measurements by Lian and co-workers for solvent-free samples (in air, under normal laboratory conditions) showed very small contribution of picosecond-time-scale ET.[8,9] Recently, the authors have noticed a more-pronounced picosecond component when the films are in contact with solvent.[18] The aforementioned discussion leads to a very contradictory picture; in some cases, there seems to be practically no environmental effects, but in other cases, there are indications that environmental conditions could influence the ET kinetics. A second factor to be discussed is the consequences of differences in the $TiO_2$ film. Lian and co-workers[8,9] used Degussa P25 $TiO_2$ powder as a starting material for $TiO_2$ paste, and the prepared films therefore contain a mixture of anatase and rutile (70:30) nanocrystals, whereas other groups have used pure anatase $TiO_2$. These two crystal forms have different

physical properties, such as band-gap energy and energy of the conduction band edge;[19] hence, the rates of ET from the dye to the nanoparticles may be different for them.[20] Furthermore, the crystal structure and quality of the $TiO_2$ films may have an effect on the ET kinetics. Normally, organic additives are used in the $TiO_2$ paste to prevent aggregation of the particles and to improve the quality of the prepared film.[1,21] These additives are removed at high temperature, normally at ∼450 °C. In the firing process, the $TiO_2$ nanoparticles form a solid interconnected network of particles with a certain size distribution.[21] The firing temperature affects also the crystallinity of the $TiO_2$ particles.[22] For nanocrystalline $TiO_2$ films, it was concluded that, by changing the firing temperature in the film preparation, the quality of the $TiO_2$ nanoparticles is altered; the higher the firing temperature, the better the crystallinity.[23] The same study also showed that the ET kinetics from Fluorescein 27 to $TiO_2$ nanoparticles is correlated to the quality of the film: the better the crystallinity of the particle, the faster the electron injection.[23] The importance of the trap/surface states on interfacial electron injection kinetics also has been observed for other sensitizer−semiconductor systems.[24,25]

As discussed previously, several parameters may influence the role of ET kinetics in RuN3-sensitized $TiO_2$ films. This complicates a comparison of the ET time constants obtained in the earlier studies.[4−16] To make a meaningful comparison of the ET kinetics measured by different authors, the differences in experimental conditions should be taken into account and their possible influence on the ET dynamics understood. In the present study, we have investigated how variations in sample preparation and measurement conditions affect the dynamics of electron injection in RuN3-sensitized $TiO_2$ films.

## 2. Experimental Section

**2.1. Sample Preparation.** *2.1.1. Sensitized Nanocrystalline $TiO_2$ Films.* The RuN3 dye (Ruthenium 535) and anatase $TiO_2$ paste (Ti-Nanoxide HT) were purchased from Solaronix SA, Switzerland. The concentration of the paste was adjusted to produce porous films with a thickness of ∼1 $\mu$m, when cellophane tape (Scotch Magic) was used as a frame for spreading. The glass substrate of the samples was an ∼80-$\mu$m-thick microscope cover slip. After spreading, the $TiO_2$ film was dried in air and sintered at ∼430 °C for 15 min in air. When the film had cooled to a temperature of ∼80 °C, it was placed for several hours in a RuN3−ethanol solution (concentration of $3 \times 10^{-4}$ M). After removal from the dye bath, the nonadsorbed dye was washed off by purging the film with ethanol and the film was dried at room temperature for ∼20 s. A spacer frame with a thickness of 0.13 mm was placed on top of the RuN3−$TiO_2$ glass sheet, together with another thin microscope cover slip, and the space between the glasses was filled with solvent (normally acetonitrile). Paper clips were used to press both glasses toward the spacer, to prevent evaporation of the solvent during measurements. The final sample had an absorbance of 0.45 ± 0.04 at 540 nm, compared to that in air. For the resonance Raman measurements, thicker $TiO_2$ films (∼4 $\mu$m) were prepared on a normal microscope glass, and these samples were inserted into a round glass container that was filled with acetonitrile. For steady-state absorption measurements, thin $TiO_2$ films with a thickness of ∼100 nm were prepared on a quartz plate.

*2.1.2. Sensitized Electron-Beam-Evaporated (EBE) $TiO_2$ Films.* Electron beam evaporation (EBE) of $TiO_2$ (Cerac T-1192) at a pressure of $5 \times 10^{-5}$ mbar was used to prepare the EBE-$TiO_2$ film on an indium tin oxide (ITO) substrate (Merck, KGaA). Using a deposition rate of 0.6−1.2 nm/s, films with a thickness of 800 ± 50 nm were produced, and these films were fired in an oven at 520 °C for 1 h. To confirm the crystal structure of the $TiO_2$, some of the film was removed from the substrate and powder X-ray diffraction (XRD) data was recorded. Details of the experimental setup is given elsewhere.[26] From the powder X-ray data, it was concluded that the $TiO_2$ crystals were anatase. The EBE films, in contrast to the sol−gel films, were not sensitized immediately after preparation; the films were kept at 100 °C for 10 min before being immersed into the RuN3 solution for several hours. Otherwise, the sample cells were prepared as described previously. For steady-state absorption measurements, a thin EBE-$TiO_2$ film (with thickness of ∼20 nm) was prepared on BK7 glass.

**2.2. Femtosecond Spectrometers for Transient Absorption Measurements.** Time-resolved differential absorption measurements were conducted in the conventional manner, and two different laser systems were used in the studies.

*2.2.1. Laser System 1.* Pump and probe pulses were provided by a noncollinear optical parametric amplifier (NOPA) that was pumped with an amplified, 1 kHz, Ti:sapphire laser system (Clark-MXR, model CPA-2001). The pump pulses ($\lambda$ = 455 or 530 nm) and probe pulses ($\lambda$ = 850 or 860 nm) were each compressed to ∼30 fs by prism compressors. The instrumental response function was determined by sum frequency cross correlation in a 30-$\mu$m-thick BBO crystal.

*2.2.2. Laser System 2.* An amplified Ti:sapphire laser (Spectra-Physics/Spitfire-Merlin)/collinear optical parametric amplifier system (Topas, Light Conversion Ltd.) was used to generate excitation (530 nm) and probe pulses of ∼100 fs with a repetition rate of 5 kHz. For probe and reference beam generation, a small portion of the laser output was used to generate a white-light continuum in a sapphire plate. Wavelengths were selected by a monochromator (with a spectral resolution of 5 nm) that was positioned after the sample. The instrument response function was determined by sum frequency cross correlation in a 200-$\mu$m-thick BBO crystal.

For all measurements, the intensity of probe, reference, and pump beams were measured by silicon photodiodes. Absorption changes as small as $10^{-5}$ could be accurately recorded. Excitation pulse intensities below ∼$10^{15}$ photons/cm$^2$ were used in the measurements, except when studying pump intensity dependency of the transient absorption signal. The precise zero-time delay between the pump and probe pulses was determined in two ways: (i) by the weak nonresonant "spike signal" in an ∼80-$\mu$m glass sheet (the thin glass sheet was identical to the substrate glass of the sample cells), and (ii) by sum frequency cross correlation in the nonlinear crystal, with the thin glass sheet inserted in the beams before the crystal position. Recorded kinetics were analyzed with deconvolution software (Spectra Solve, version 3.01 PRO, Ames Photonics, Inc.), and fits of the oscillatory curves were performed with Mathematica 4.0.1.0 (Wolfram Research, Inc.) and Fourier transforms with c++ program (fast Fourier transform (FFT), Hamming windowing).

**2.3. Raman Measurements.** The Raman measurements were performed in the 100−3000 cm$^{-1}$ region, using a single-stage spectrometer (Acton SpectraPro 500I, resolution of 10 cm$^{-1}$) that was equipped with a 1024 × 256 pixel charge-coupled device (CCD) camera (Andor InstaSpec IV). The radiation of an $Ar^+$ laser (Omnichrome 543-AP, 488 nm) was directed toward a film at an angle of ∼45° in P-polarization and focused to an ∼50-$\mu$m spot. The Raman scattered light was transmitted without polarization analysis through collecting optics, a

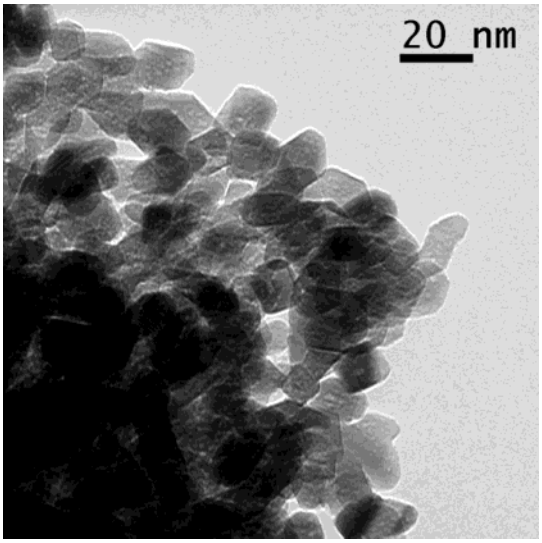


**Figure 1.** Transmission electron microscopy (TEM) image of a nanocrystalline $TiO_2$ film. Estimated average diameter of the nanoparticles is $10 \pm 3$ nm.

holographic filter (Kaiser Super-Notch-Plus), and an optical fiber. No degradation of the films was observed on irradiation.

**2.4. Steady-State Absorption Measurements.** An ultraviolet/visible (UV/vis) spectrophotometer (Jasco, model V-530) was used to ensure that samples were not degraded during preparation or laser experiments. It was also used to study the degradation of the RuN3−$TiO_2$ in air and the absorption spectra of thin $TiO_2$ films.

**2.5. Transmission Electron Microscopy (TEM) Measurements.** The samples were investigated via transmission electron microscopy (TEM) (model JEM 2000FX). The microscope has a resolving power of 2.7 Å at 200 kV and is equipped with a slow-scan CCD camera for direct digital recording as well as traditional photographic film. The $TiO_2$ films were removed from the glass substrate, gently grinded, and then dispersed onto holey carbon-coated copper grids by dipping them in methanol. The average sizes of the $TiO_2$ particles and voids were determined from TEM photographs.

## 3. Results and Discussion

As discussed in the Introduction, several parameters can influence the electron transfer (ET) kinetics of the RuN3-sensitized $TiO_2$ films, necessitating a careful definition of a reference system. This includes materials for preparation of the $TiO_2$ film and the environment of the sensitized film, as well as the characteristics of the transient absorption setup (pump photon density, excitation and probe wavelengths). Here, we will give a complete characterization of the reference sample and its transient absorption kinetics, followed by a study of how the kinetics is changed as a result of variations in sample preparation or experimental conditions.

**3.1. Characterization of the Reference Sample and Kinetics.** Recently, we performed detailed studies on the ET kinetics of RuN3-sensitized nanocrystalline $TiO_2$ films in acetonitrile.[14,15] The sample used in those studies will be the reference in the present study. The $TiO_2$ film that was prepared from the Solaronix Ti-nanoxide HT paste is highly transparent, and the average size of the nanoparticles in the film was measured to be $10 \pm 3$ nm via TEM. A typical TEM image is shown in Figure 1.

Despite the high transparency of the $TiO_2$ film and good absorbance (~0.45) of the RuN3, the nonlinear coherent

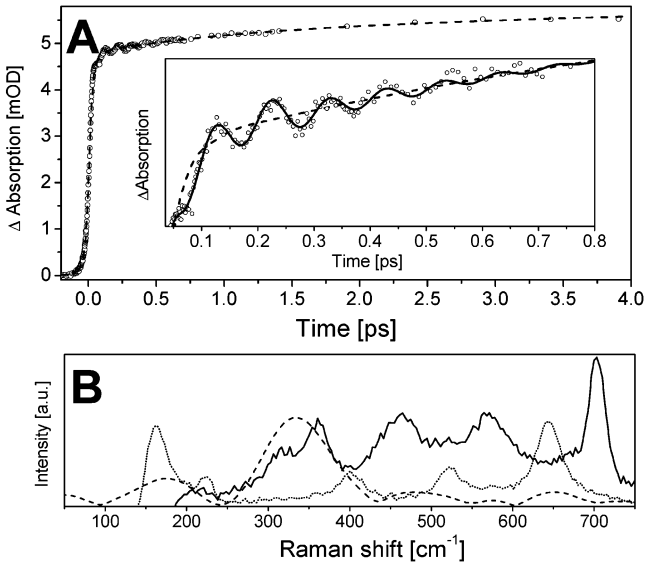


**Figure 2.** (A) Oscillations in the transient absorption signal of a RuN3-sensitized nanocrystalline $TiO_2$ film (reference sample); the kinetics at 850 nm is plotted (open circles), together with a multiexponential fit (dashed line). (In the inset, the solid line shows a fit of the kinetics after adding two exponentially damped cosine functions ($\omega_1 = 330$ $cm^{-1}$ and $\tau_1 = 240$ fs, and $\omega_2 = 175$ $cm^{-1}$ and $\tau_2 = 112$ fs) to the multiexponential fit (represented by the dashed line)). (B) Comparison between (•••) the Raman spectrum of $TiO_2$ film in acetonitrile, (—) the Raman spectrum of RuN3−$TiO_2$ in acetonitrile, and (- - -) Fourier transform of the oscillatory signal.

coupling signal between the pump and probe pulses may distort the initial portion of the recorded transient absorption kinetics. To allow measurements of weak signals near zero time, thin glass sheets (~80 $\mu$m thick) were used as the substrate and cover sheets. Using these glass sheets, together with a thin spacer (~0.13 mm), and positioning the sensitized film toward the incoming laser beam, we were able to reduce the coherent coupling signals below our detection limit.

The recorded kinetics of the reference sample is dependent on the excitation wavelength and the spectral position of the probe pulses.[14,15] All kinetics presented in this study are recorded with an excitation at 530 nm and probing at 850 or 860 nm. Earlier studies have shown that the induced absorption signal in this probe wavelength region is complex and contains contributions from the RuN3 cation, excited-state absorption, and a weak absorption of injected electrons in the conduction band of the $TiO_2$.[4,6,14,27,28] In our earlier study, the nonexponential kinetics at 860 nm that shows the formation of $RuN3^+$ was well-fitted with the following time constants and amplitudes (the latter given in parentheses): instantaneous rise within the laser pulse (20%), 28 fs (50%), 1 ps (11%), 9.5 ps (12%), and 50 ps (7%).[14] The instantaneous rise (20%) is due to initially populated singlet excited-state absorption and the rest (80% of the full amplitude) is attributed to electron injection from the singlet (28 fs) and triplet excited states (picosecond-time-scale components).[14]

In the earlier reported data,[14,15] we already observed small oscillations in the kinetics; these oscillations are now the subject of further study. A low-amplitude oscillation in the transient absorption signal at 850 nm is observed for time delays shorter than ~0.6 ps after excitation (see panel A in Figure 2).

To quantify these oscillations, the transient signal was fitted with a sum of exponentials and the residuals that contained the oscillations was further analyzed with two different methods: by fitting with exponentially damped cosine functions and by Fourier transform analysis.

For the damped cosine fit, the formula

$$f(t) = \sum_{i=1}^{n} A_i \cos(\omega_i t + \theta_i) \exp\left(-\frac{t}{\tau_i}\right)$$

was used, where $A_i$ is the initial amplitude, $\omega_i$ the frequency, $\theta_i$ the phase of the cosine function being characterized by the damping time ($\tau_i$). A good fit was obtained using two oscillating components with the optimized frequencies and damping times of (i) $\omega_1 = 330$ cm$^{-1}$ and $\tau_1 = 240$ fs and (ii) $\omega_2 = 175$ cm$^{-1}$ and $\tau_2 = 112$ fs. A fit, where these damped oscillations are added to the multiexponential fit of the kinetics, is shown in the inset of Figure 2A. The measured data are nicely fitted throughout the displayed time window of 0−0.8 ps; for times longer than ~0.6 ps, the oscillations are washed out by the noise of the recorded signal. Fourier analysis of the oscillations shows a pronounced peak at 335 cm$^{-1}$ and a small peak at 175 cm$^{-1}$ (Figure 2B), which is in good agreement with the exponentially damped cosine fitting. The smaller peaks in the Fourier transform spectrum are close to the noise level.

The fitted Fourier transformed frequencies were compared with the frequencies obtained from the resonance Raman spectrum of RuN3-sensitized $TiO_2$ in acetonitrile. The low-frequency region (150−750 cm$^{-1}$) of the resonance Raman spectrum is shown in Figure 2B, together with the Fourier transform spectrum of the oscillatory signal and Raman spectrum of $TiO_2$ film in acetonitrile. Comparison of the spectra shows that the resonance Raman peaks at 320 and 360 cm$^{-1}$ practically coincide with the pronounced peak obtained from the Fourier analysis. The Raman spectra of RuN3 in ethanol, the "naked" $TiO_2$ film in acetonitrile, and the solvents (ethanol and acetonitrile) confirmed that the two peaks are due to vibrations of the RuN3 molecule. This assignment is in good agreement with earlier Raman studies of bis(tetrabutylammonium) Ru(dcbpy)$_2$(NCS)$_2$ (which is referenced as N719) and Ru(bpy)$_3$ molecules.[29,30] According to ab initio calculations of RuN3 under vacuum, the dcbpy ligand and also the ruthenium participates in the vibrational modes in the region of 300−400 cm$^{-1}$.[31]

The fitted damping time of the most-pronounced oscillation was ~240 fs, which is clearly longer than the ET from the singlet state (~50 fs) or ISC (~75 fs).[14,15] It is not clear from these data, whether the vibrational wave packet generated in the donor state (singlet excited dye) continues its motion in the product (dye cation) state of the reaction, as suggested by Willig and co-workers[32,33] for the perylene−$TiO_2$ system, or whether it continues its motion in the triplet excited state of RuN3 after ISC. Similar oscillations were observed for RuN3 in ethanol (data not shown), and, thus, it is only concluded that the vibrational wave packet survives longer than the singlet-state ET process and ISC.

**3.2. Influence of Pump Intensity.** An essential parameter in transient absorption measurements is the photon density of the pump pulses. To obtain correct kinetics, a linear response of the signal as a function of pump intensity must be achieved. For the reference sample, the amplitude of the transient absorption signal increased linearly, up to a photon density of $3 \times 10^{15}$ photons/cm$^2$ per pulse, with an excitation at 530 nm (both induced absorption and bleaching signals were examined). This is in good agreement with most of the earlier studies, where typically ~$2 \times 10^{15}$ photons/cm$^2$ or less have been used for pumping.[4,8,9,11,13−16] If the sample was excited with photon densities of $>10^{16}$ photons/cm$^2$ per pulse, a decay of the induced absorption measured at 860 nm was observed, instead of an increase in the signal, as was recorded at lower intensities (Figure 3). It can be suggested that this decay could result from light-induced degradation of the RuN3 or acceleration of the backelectron transfer (BET) or annihilation processes. The first explanation, light-induced degradation of the dye, is supported by the observation that the signal was not reproducible and translation of the sample decreased the decay amplitude of the signal (see Figure 3) and increased the overall magnitude of the signal considerably (by ~40%). Thus, keeping the sample fixed and irradiating it at the same spot for several minutes results in substantial sample degradation. The second possible reason for decay of the signal is fast BET from the conduction band/trap states of the $TiO_2$ to the $RuN3^+$ cation. In many studies, BET is reported to occur nonexponentially on the microsecond and millisecond time scale, with only a negligible contribution from picosecond-time-scale or nanosecond-time-scale components.[4,11,34−37] However, the BET kinetics is dependent on excitation intensity: Durrant et al. reported that BET kinetics is independent of excitation intensity only with low photon densities ($\leq 3 \times 10^{14}$ photons/cm$^2$ per pulse) when approximately one electron per $TiO_2$ particle is present.[36] When the excitation pulse intensity was increased from ~$3 \times 10^{14}$ photons/cm$^2$ to ~$2 \times 10^{16}$ photons/cm$^2$, they observed nonlinear behavior of the BET kinetics and an increased rate of recombination (by a factor of at least $10^3$), and a significant portion of the BET started to occur on time scales less than the time resolution of the experiment, i.e., faster than 100 ns.[36] Thus, BET might extend to time domains less than a nanosecond, and some portion of the measured decay at high pump intensity could originate from recombination processes. Yet, the observed ~20% decay of the $RuN3^+$ absorption signal that occurs during the first 1−2 ps most probably does not represent the short-time wing of a single smooth distribution of BET rates. To be considered as BET, this decay should be caused by a new mechanism of fast recombination. A third possibility for the decay of the signal at high photon density is annihilation.[38−40] However, in the present case, this is not a likely reason, because annihilation is not expected to decrease the concentration of $RuN3^+$ cations probed at 860 nm. Annihilation of the remaining triplet excited states would not account for the observed decay (more than 30% at the highest excitation intensity), because the maximum contribution of the triplet-induced absorption to the signal is <10%.

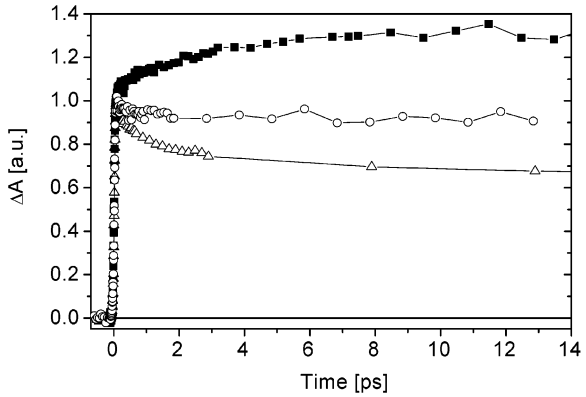


**Figure 3.** Influence of pump intensity. Normalized transient absorption kinetics at 860 nm with excitation intensities of (■) $3 \times 10^{15}$ and (○,△) $2 \times 10^{16}$ photons/cm$^2$ per pulse (open circles represent data from the translated sample and open triangles represent data from the stationary sample). With high intensities, a decay of the transient absorption signal was observed instead of an increase, as was measured with low-excitation photon densities.

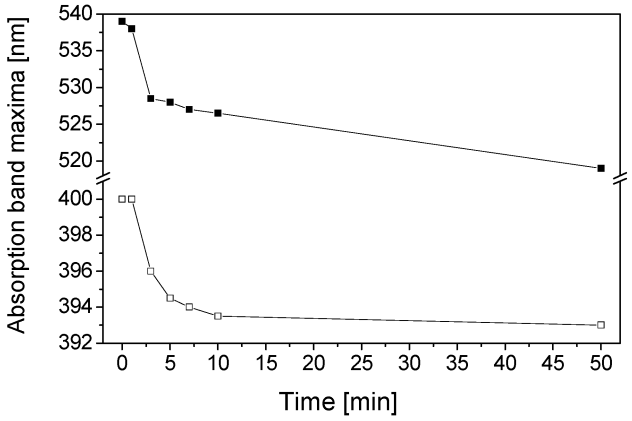


**Figure 4.** Shift of the two RuN3 steady-state main absorption band maxima as a function of exposure time to ambient air.

To summarize this part of the work, when RuN3−$TiO_2$ films are excited with high photon densities (outside the region of the linear response), the kinetics is changed in the picosecond time domain and the corresponding processes are most likely related to photodegradation of RuN3 and possibly to BET in the picosecond time domain. In the first case, the observed kinetics is unrelated to ET.

**3.3. Influence of Environment of the Sensitized Film.** Samples to be discussed below were prepared in the same manner as the reference sample, with the exception that the environment (solvent) of the sensitized film was changed.

*3.3.1. Normal Laboratory Conditions.* We observed that, during the sample preparation, it was essential not to expose the prepared RuN3−$TiO_2$ film to ambient air for a long time. When RuN3-sensitized $TiO_2$ samples were kept in air, a change in sample color was observed. The steady-state absorption spectrum of freshly prepared RuN3 on nanocrystalline $TiO_2$ film shows two main absorption bands in the visible spectral region, with maxima at 539 nm and 400 nm. When the sensitized film was exposed to air, the absorption bands started to blue-shift. Five minutes after the RuN3-sensitized film was removed from the acetonitrile solvent, the absorption band maxima at 539 nm (400 nm) had blue-shifted by 10 nm (5 nm) from the initial values and 19 nm (7 nm) after 50 min (see Figure 4). Because some of the earlier measurements for the RuN3−$TiO_2$ system were performed under normal laboratory conditions with the sample in contact with air,[8,9] we measured how shifts of the steady-state absorption bands are correlated to the transient absorption kinetics. In Figure 5, we show a comparison between kinetic data measured for a sample in acetonitrile and a sample in air. The RuN3-sensitized film was the same in all experiments; however, the cover glass sheet and acetonitrile solvent were removed after the first measurement and several kinetic traces were recorded subsequently. Because recording of a single transient absorption trace takes ∼2 min, only the starting time of each measurement is shown in the figure.

Comparison between the traces shows that the amplitudes of the slower picosecond-rise-time components decrease as the sample is exposed for increasingly longer times to air. At the beginning (sample in acetonitrile), the total percentage amplitude of the picosecond-rise-time components was 29%, and under continuous exposure to air, it changed to 23% (0 min), 13% (3 min), and 8% (5 min), and after 7 min, the picosecond-rise-time signal had already changed to a decay. These changes are also illustrated by measuring the transient absorption signal of the sensitized film in air at a fixed time delay of 12 ps (see inset of Figure 5): the signal decreased almost linearly, at a

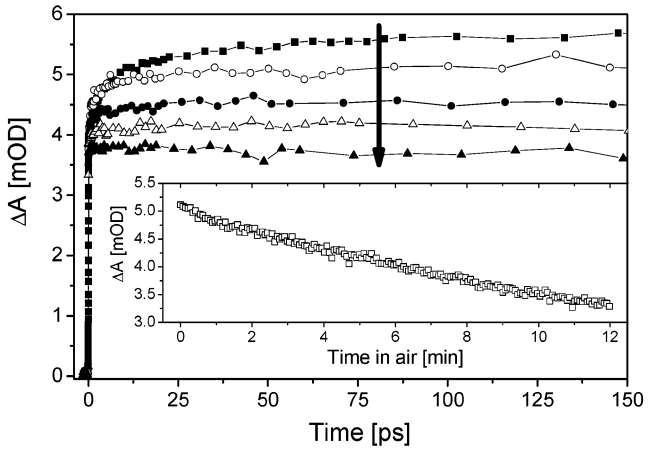


**Figure 5.** Effect of exposure to air on the transient absorption kinetics of the RuN3-sensitized $TiO_2$ films at 850 nm in acetonitrile ((■) reference sample) and (○) 0 min, (●) 3 min, (△) 5 min and (▲) 7 min after the acetonitrile was removed from the sample cell. A gradual decrease of the picosecond-time-domain rise components is observed for increasing air exposure. Inset shows the decrease of the induced absorption with time at a fixed delay time of 12 ps.

rate of ∼0.14 mOD/min, showing the disappearance of the rise components. In this measurement (Figure 5), the position of the sample was kept fixed and, thus, both air and light can contribute to the decrease of the signal. It has been reported that decomposition of the dye in air is significantly accelerated by irradiation with visible light.[6,41]

From this observation, we conclude that, to avoid degradation, the RuN3-sensitized film must be protected from ambient air by an inert environment, such as a solvent. It is evident that the moment the RuN3-sensitized film is exposed to air, the absorption spectrum starts to blue-shift, and this has a dramatic effect on the measured transient absorption kinetics at 860 nm. Therefore, during preparation of the samples, the sensitized $TiO_2$ films were kept for times that were as short as possible in air (∼20 s), and the freshness of the sample was always tested before experiments by steady-state absorption measurement. If, for some reason, the maxima of the absorption bands were blue-shifted, the sample was not used in the measurements. A similar type of degradation of the sample could be observed by keeping the film in a dye bath for several days. In the present study, low amplitudes of picosecond-time-scale ET is correlated with spectral changes of the sample; therefore, it was related mostly to degradation of the dye, rather than to changes in the ET kinetics. This observation indicates that differences in the environment of the dye-sensitized film might explain some of the differences in the earlier reported picosecond-rise-time kinetics.

*3.3.2. Solvent Effect.* As discussed previously, the solvent protects the sample from degradation; however, it also might have an influence on the measured kinetics. To investigate this effect, we measured the kinetics of the RuN3−$TiO_2$ film in both acetonitrile and 3-methoxypropionitrile (3-MPN). A comparison of the observed ET kinetics of RuN3−$TiO_2$ film in these solvents is shown in Figure 6. A clear difference in the kinetics is observed, and the total percentage contribution of the picosecond-time-scale components (time constants of 1, 9.5, and 50 ps) is 29% in acetonitrile, whereas in 3-MPN, it is 19%. When the traces are scaled to the same amplitude at 100 fs (see inset in Figure 6), the identical triplet excited-state electron injection kinetics is obvious. This shows that the picosecond time constants of ET are not changed, which indicates that the picosecond ET processes could be controlled by intramolecular

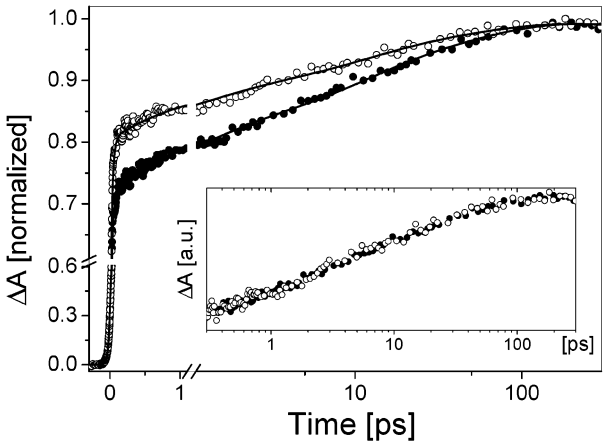


**Figure 6.** Influence of solvent. Transient absorption kinetics of the RuN3-sensitized film at 850 nm in different solvent environments ((●) in acetonitrile and (○) in 3-methoxypropionitrile (3-MPN)). The total amplitude of the fitted picosecond time constants (1, 9.5, and 50 ps) is 29% in acetonitrile and 19% in 3-MPN. Inset: Scaled kinetics show that the same time constants fit the data in both solvents (scaled to the same signal size at delay times of 0.1 and 300 ps).

dynamics of the RuN3 dye.[42] The observed change in the relative amplitudes might be caused by a difference in the extinction coefficients of $RuN3^+$ and/or RuN3* at 850 nm in acetonitrile and 3-MPN. In addition, changes in energetic positions of the electronic donor/acceptor states might also occur,[43] which leads to different ratios of the singlet and triplet channels of ET. Here, it suffices to say that different solvents may cause variations in ET kinetics, but a more-detailed, systematic study is required to draw further conclusions.[44]

**3.4. Influence of $TiO_2$ Film Preparation.** For the samples to be discussed below, the preparation of the electron-accepting $TiO_2$ film was changed while other sample properties were maintained the same as in the reference sample.

*3.4.1. Firing Temperature.* It has been reported that the firing temperature affects the physical properties of the $TiO_2$ nanoparticles, and the corresponding changes can be monitored by steady-state absorption spectroscopy. In the linear absorption spectrum of the nanocrystalline $TiO_2$ films, the UV spectral region is dominated by indirect and direct band transitions of the semiconductor, whereas the absorption in the visible region is due to the states below the conduction band edge, which are attributed to various defects.[22,23,45−47] To measure the absorption spectrum of the $TiO_2$ film in the visible and UV regions simultaneously, the prepared films must be ultrathin, because of the high extinction coefficient of the $TiO_2$ in the UV region. Two identical films with a thickness of ~0.1 $\mu$m were prepared and fired at 300 °C and at 450 °C, respectively. A comparison of the measured steady-state absorption spectra of the films is shown in Figure 7.

For the sample that was prepared at a high firing temperature (450 °C), a lower absorption in the visible region is obtained, in comparison to the sample that was fired at 300 °C. This can be attributed to a smaller amount of defects and, consequently, better crystallinity of the nanoparticles.[22,23,45−47] An influence of the firing temperature is observable also after sensitization (see absorption spectra in the inset of Figure 7). The absorbance of the RuN3−$TiO_2$ film is lower in the sample that was fired at high temperature (450 °C). This observation is similar to that of a recently reported study of Fluorescein 27-sensitized $TiO_2$ films,[23] where the lower absorption of the dye was attributed to an increase of nanoparticle and pore sizes at high firing temperatures, which leads to a decrease of the internal surface

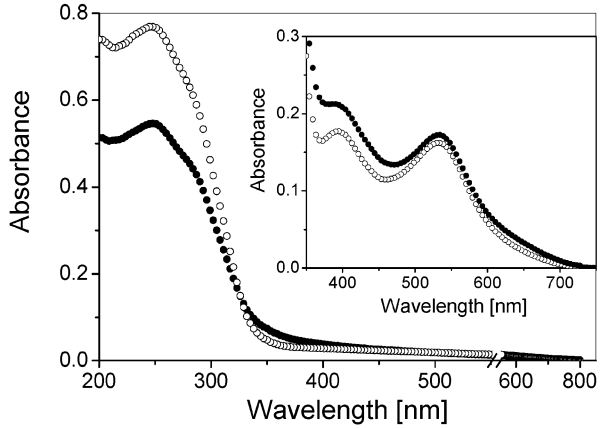


**Figure 7.** Comparison of steady-state absorption spectra of two identical $TiO_2$ films after firing ((○) at 450 °C (reference sample) and (●) at 300 °C). Inset shows the absorption spectrum after sensitization with RuN3.

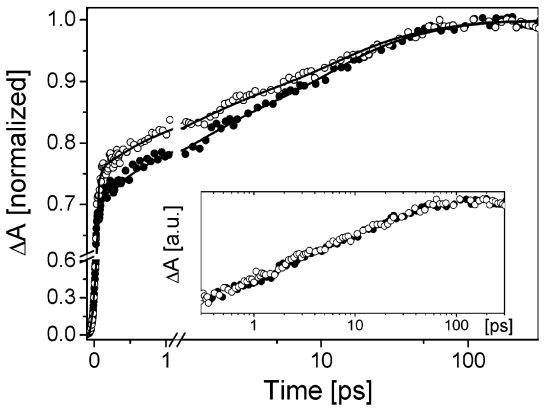


**Figure 8.** Influence of $TiO_2$ firing temperature, showing a comparison of the normalized transient absorption kinetics of two RuN3-sensitized identical $TiO_2$ films fired (○) at 450 °C (reference sample) and (●) at 300 °C. Inset: Scaled traces show that the time constants in both cases are identical (scaled to the same signal size at delay times of 0.1 and 300 ps).

area and, consequently, to a smaller amount of adsorbed dye in the film.[21−23,48,49] The same phenomenon is expected to produce the observed spectral changes shown in the inset of Figure 7.

To determine how the film quality influences the ET, the transient absorption kinetics of the two differently fired sensitized films were measured. A comparison of the kinetics (Figure 8) shows that there is a small decrease in the relative amplitudes of the picosecond components of the sample fired at the higher temperature. This is qualitatively verified by an exponential fit, which yields the same picosecond lifetimes as we have used previously in this work (1, 9.5, 50 ps) for both traces, only a small decrease from 31% to 26%−29% of the total amplitude of the picosecond components was observed when going from a firing temperature of 300 °C to 450 °C.

The insensitivity of ET lifetimes to firing temperature (also shown by the scaled kinetics of the inset in Figure 8) is another indication that the picosecond lifetimes do not directly represent the ET step, but are more controlled by RuN3 intramolecular relaxation processes in the triplet state.[42,50]

*3.4.2. Electron-Beam-Evaporated $TiO_2$ Film.* To study further the influence of band-gap states on the ET kinetics, we used electron beam evaporation (EBE) to produce an anatase $TiO_2$ film with special characteristics. TEM images of an EBE-$TiO_2$ film showed a structure that was very different from that of films made of nanocrystalline particles. The surface of the EBE

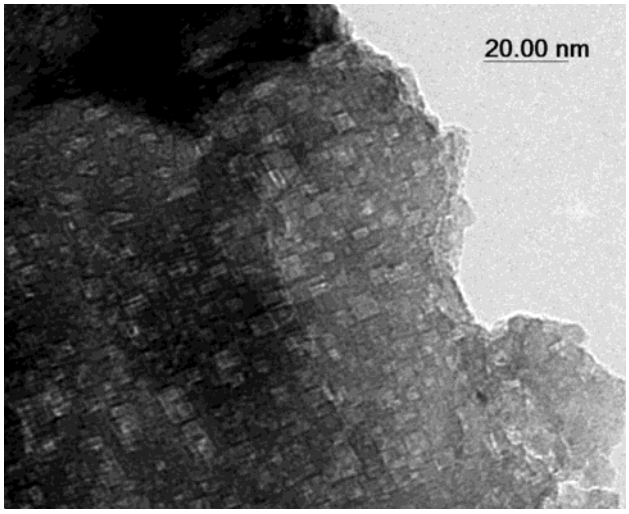


**Figure 9.** TEM image of the electron-beam-evaporated (EBE) $TiO_2$ film. The average size of the rectangular voids was estimated to be (5 ± 2) nm × (7 ± 4) nm.

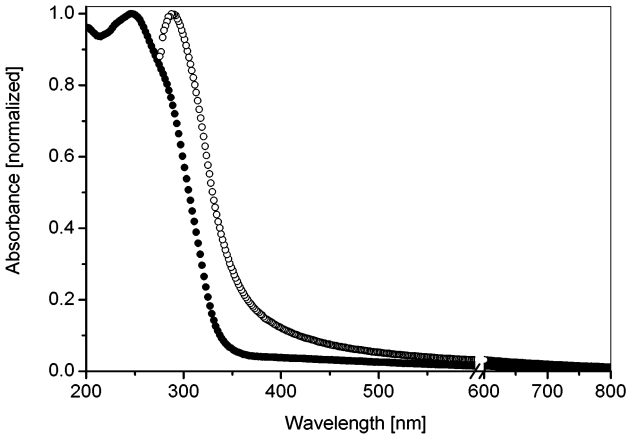


**Figure 10.** Comparison between normalized steady-state absorption spectra of (○) EBE-$TiO_2$ film and (●) nanocrystalline $TiO_2$ film. The EBE-$TiO_2$ film has substantial absorption in the visible (vis) and near-UV region. The absorption spectrum of the EBE film is shown only up to 275 nm, because of the high absorption of the BK7 glass substrate material.

films contained rectangular voids with average dimensions of 5 ± 2 nm × 7± 4 nm (Figure 9), similar to what has been observed previously in $TiO_2$ material, which was intended as catalysis support.[51]

Because of the defects, the EBE film has a nanostructure, which leads to a reasonable optical density (∼0.13 at 540 nm) of a 0.8-$\mu$m-thick film after sensitization. To obtain information about the amount of defect states in the EBE film, the steady-state absorption spectrum of a ∼20-nm-thick film was measured and compared with the spectrum of the aforementioned ultrathin nanocrystalline $TiO_2$ sample (fired at 450 °C) (see Figure 10). The EBE film has significant absorption both in the vis and near-UV regions, showing that a large amount of band-gap states is present in this film.

The transient absorption kinetics of the RuN3-sensitized EBE film was measured, and a comparison with the kinetics of the reference sample (Figure 11) shows that the ET process is significantly slower in the RuN3-EBE sample. The increase of the RuN3-EBE signal was fitted with the following time constants and amplitudes: instantaneous rise within the laser pulse (45%), 0.20 ps (27%), 1.1 ps (7%), and 10 ps (21%). In contrast to the ET kinetics of the reference nanocrystalline film,

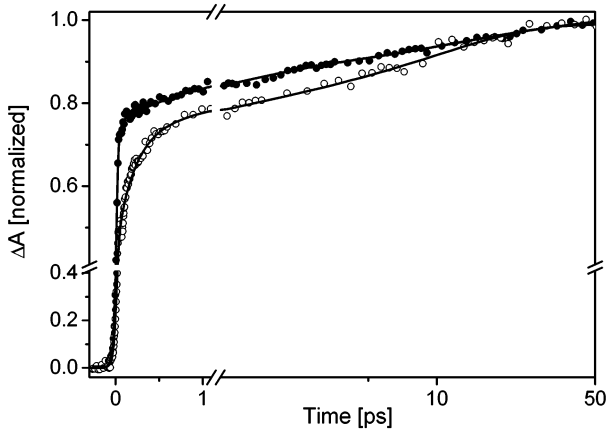


**Figure 11.** Transient absorption kinetics at 850 nm in (○) the RuN3-sensitized EBE-$TiO_2$ film and (●) the nanocrystalline $TiO_2$ film (reference sample). Solid line represents the kinetics of the sensitized EBE film fitted with the following time constants and amplitudes (given in parentheses): instantaneous rise within the laser pulse (45%), 0.20 ps (27%), 1.1 ps (7%), and 10 ps (21%).

a major portion of the kinetics occurs after 100 fs (≥55%) and a new time constant of 200 fs was needed to fit the data properly. In the reference sample, ISC occurs in ∼75 fs and the fastest time constant for triplet excited-state electron injection is 1 ps.[14,15] Provided that the film morphology does not influence the ISC rate of the sensitizer, the new 200-fs ET process must originate from the triplet excited state of RuN3. Thus, the EBE-$TiO_2$ film sensitized with RuN3 is characterized by a lower fraction of electron injection from the singlet state and an additional, faster (200-fs) injection process from the triplet state, in comparison to that of the conventional nanocrystalline film. The small fraction of singlet injection can be explained as a morphology-induced decrease of ET rate from the RuN3 singlet state in the EBE film, and, thus, a higher population of the RuN3 triplet state is formed. A change in electron injection rate could be caused by many reasons: a different binding geometry at different crystal sites (on the top of the film and inside the voids); a change in the electronic coupling strength (different crystal surfaces); a varied density of electron-acceptor levels (different crystallinity); and contamination of the film surface (the EBE film was not sensitized immediately after preparation). The additional 200-fs electron injection pathway could also be a result of special binding geometry of RuN3 to the EBE film. A fraction of the RuN3 molecules may bind to the EBE film via three or four carboxylate groups, rather than via two carboxylate groups, as reported for nanocrystalline $TiO_2$ samples.[52,53] This special binding may occur at intersections of crystal planes (at the inner edges of the voids) and eventually lead to a higher rate of ET from the RuN3 triplet state.

## 4. Conclusions

We have investigated the influence of sample preparation parameters and environmental conditions on the electron injection dynamics of RuN3-sensitized nanocrystalline $TiO_2$ films. All measured kinetics were compared to a well-defined reference sample for which detailed studies have been reported here and previously.[14,15] The induced effects on the transient absorption kinetics were quite small, when firing temperature of the $TiO_2$ film or the solvent environment of the sample was changed. The differences in these parameters might explain only small variations in the earlier reported time constants and amplitudes. On the contrary, high excitation photon density, exposure of the RuN3-sensitized film to air, or preparation of the $TiO_2$ film

by electron beam evaporation induce substantial effects, especially some in the picosecond-time-domain kinetics. According to our results, many modifications of the sample and experimental conditions affect the transient absorption kinetics. The differences in the kinetics reported earlier by different groups might be partially due to variance in the aforementioned conditions. The conclusion is supported by a recent study by Asbury et al., where the effect of excitation wavelength and solvent environment of the sample on the electron injection kinetics was investigated.[54]

**Acknowledgment.** We thank Dr. M. Lahtinen (University of Jyväskylä) for help with the powder X-ray measurements and interpretation of the X-ray data. This research was funded by grants from the Academy of Finland (under Contract No. 44546) and by the graduate school LASKEMO, Delegationen för Energiförsörjning i Sydsverige (DESS), the Swedish Research Council, the Knut and Alice Wallenberg Foundation, the Royal Physiographic Society in Lund, the Crafoord Foundation, the Trygger Foundation, the European Community (under Contract Nos. HPRI-CT-1999-00041 and ERBFMGECT950020), and the European Science Foundation (ULTRA program).

## References and Notes

(1) Nazeeruddin, M. K.; Kay, A.; Rodicio, I.; Humphry-Baker, R.; Müller, E.; Liska, P.; Vlachopoulos, N.; Grätzel, M. *J. Am. Chem. Soc.* **1993**, *115*, 6382.

(2) Hinsch, A.; Kroon, J. M.; Kern, R.; Uhlendorf, I.; Holzbock, J.; Meyer, A.; Ferber, J. *Prog. Photovoltaics: Res. Appl.* **2001**, *9*, 425.

(3) Kohle, O.; Grätzel, M.; Meyer, A. F.; Meyer, T. B. *Adv. Mater.* **1997**, *9*, 904.

(4) Tachibana, Y.; Moser, J. E.; Grätzel, M.; Klug, D. R.; Durrant, J. R. *J. Phys. Chem.* **1996**, *100*, 20056.

(5) Hannappel, T.; Burfeindt, B.; Storck, W.; Willig, F. *J. Phys. Chem. B* **1997**, *101*, 6799.

(6) Moser, J. E.; Noukakis, D.; Bach, U.; Tachibana, Y.; Klug, D. R.; Durrant, J. R.; Humphry-Baker, R.; Grätzel, M. *J. Phys. Chem. B* **1998**, *102*, 3649.

(7) Hannappel, T.; Zimmermann, C.; Meissner, B.; Burfeindt, B.; Storck, W.; Willig, F. *J. Phys. Chem. B* **1998**, *102*, 3651.

(8) Ellingson, R. J.; Asbury, J. B.; Ferrere, S.; Hirendra, N. G.; Sprague, J. R.; Lian, T.; Nozik, A. J. *J. Phys. Chem. B* **1998**, *102*, 6455.

(9) Asbury, J. B.; Ellingson, R. J.; Ghosh, H. N.; Ferrere, S.; Nozik, A. J.; Lian, T. *J. Phys. Chem. B* **1999**, *103*, 3110.

(10) Durrant, J. R.; Tachibana, Y.; Mercer, I. P.; Moser, J. E.; Grätzel, M.; Klug, D. R. *Z. Phys. Chem.* **1999**, *212*, 93.

(11) Tachibana, Y.; Haque, S. A.; Mercer, I. P.; Durrant, J. R.; Klug, D. R. *J. Phys. Chem. B* **2000**, *104*, 1198.

(12) Heimer, T. A.; Heilweil, E. J.; Bignozzi, C. A.; Meyer, G. J. *J. Phys. Chem. A* **2000**, *104*, 4256.

(13) Kallioinen, J.; Lehtovuori, V.; Myllyperkiö, P.; Korppi-Tommola, J. *Chem. Phys. Lett.* **2001**, *340*, 217.

(14) Benkö, G.; Kallioinen, J.; Korppi-Tommola, J. E. I.; Yartsev, A. P.; Sundström, V. *J. Am. Chem. Soc.* **2002**, *124*, 489.

(15) Kallioinen, J.; Benkö, G.; Sundström, V.; Korppi-Tommola, J. E. I.; Yartsev, A. P. *J. Phys. Chem. B* **2002**, *106*, 4396.

(16) Tachibana, Y.; Nazeeruddin, M. K.; Grätzel, M.; Klug, D. R.; Durrant, J. R. *Chem. Phys.* **2002**, *285*, 127.

(17) Asbury, J. B.; Hao, E.; Wang, Y.; Ghosh, H. N.; Lian, T. *J. Phys. Chem. B* **2001**, *105*, 4545.

(18) Asbury, J. B.; Hao, E.; Lian, T. unpublished results. (Discussed in *J. Phys. Chem. B* **2001**, *105*, 4545.)

(19) Kavan, K.; Grätzel, M.; Gilbert, S. E.; Klemenz, C.; Scheel, H. J. *J. Am. Chem. Soc.* **1996**, *118*, 6716.

(20) The classical ET theory qualitatively accounts for the trends of ultrafast ET reactions in the dye-sensitized semiconductor. According to nonadiabatic Marcus ET theory implemented on such dye-sensitized nanoparticles, the rate of electron injection is determined by the electron coupling between the dye and the semiconductor, the density of acceptor states in the semiconductor coupled to the dye, and the potential energy difference between the dye excited state and conduction band of the semiconductor (i.e., the driving force).

(21) Barbé, C.; Arendse, F.; Comte, P.; Jirousek, M.; Lenzmann, F.; Shklover, V.; Grätzel, M. *J. Am. Ceram. Soc.* **1997**, *80*, 3157.

(22) Hanley, T. L.; Luca, V.; Pickering, I.; Howe, R. F. *J. Phys. Chem. B* **2002**, *106*, 1153.

(23) Benkö, G.; Skårman, B.; Wallenberg, R.; Hagfeldt, A.; Sundström, V.; Yartsev, A. P. *J. Phys. Chem. B* **2003**, *107*, 1370.

(24) Hao, E.; Anderson, N. A.; Asbury, J. B.; Lian, T. J. *J. Phys. Chem. B* **2002**, *106*, 10191.

(25) Huber, R.; Spörlein, S.; Moser, J. E.; Grätzel, M.; Wachtveitl, J. *J. Phys. Chem. B* **2000**, *104*, 8995.

(26) Lahtinen, M.; Valkonen, J. *Chem. Mater.* **2002**, *14*, 1812.

(27) Das, S.; Kamat, P. V. *J. Phys. Chem. B* **1998**, *102*, 8954.

(28) Rothenberger, G.; Fitzmaurice, D.; Grätzel, M. *J. Phys. Chem.* **1992**, *96*, 5983.

(29) Webb, M. A.; Knorr, F. J.; McHale, J. L. *J. Raman Spectrosc.* **2001**, *32*, 481.

(30) Greijer, H.; Lingren, J.; Hagfeldt, A. *J. Phys. Chem. B* **2001**, *105*, 6314.

(31) Kallioinen, J., unpublished ab initio calculation of RuN3 dye in a vacuum with 3-21G* basis set in the Gaussian98 program.

(32) Willig, F.; Zimmermann, C.; Ramakrishna, S.; Storck, W. *Electrochim. Acta* **2000**, 4565.

(33) Zimmermann, C.; Willig, F.; Ramakrishna, S.; Pettinger, B.; Burfeindt, B.; Biswas, N.; Eichberger, R. *Springer Ser. Chem. Phys.* **2001**, *66*, 453.

(34) Haque, S. A.; Tachibana, Y.; Klug, D. R.; Durrant, J. R. *J. Phys. Chem. B* **1998**, *102*, 1745.

(35) Nelson, J.; Haque, S. A.; Klug, D. R.; Durrant, J. R. *Phys. Rev. B* **2001**, *63*, 205321.

(36) Haque, S. A.; Tachibana, Y.; Willis, R. L.; Moser, J. E.; Grätzel, M.; Klug, D. R.; Durrant, J. R. *J. Phys. Chem. B* **2000**, *104*, 538.

(37) Pelet, S.; Moser, J. E.; Grätzel, M. *J. Phys. Chem. B* **2000**, *104*, 1791.

(38) van Grondelle, R.; Dekker, J. P.; Gillbro, T.; Sundström, V. *Biochim. Biophys. Acta* **1994**, *1187*, 1.

(39) Wang, Y.; Asbury, J. B.; Lian, T. *J. Phys. Chem. A* **2000**, *104*, 4291.

(40) Qu, P.; Meyer, G. J. *Electron Transfer in Chemistry*; Balzani, V., Mallouk, T. E., Eds.; Wiley-VCH: Weinheim, Germany, 2001.

(41) Greijer Agrell, H.; Lindgren, J.; Hagfeldt, A. *Sol. Energy* **2003**, *75*, 169.

(42) Benkö, G.; Myllyperkiö, P.; Pan, J.; Yartsev, A. P.; Sundström, V. *J. Am. Chem. Soc.* **2003**, *125*, 1118.

(43) Redmond, G.; Fitzmaurice, D. *J. Phys. Chem.* **1993**, *97*, 1426.

(44) Myllyperkiö, P.; Benkö, G.; Kallioinen, J.; Korppi-Tommola, J. E. I.; Yartsev, A. P.; Sundström, V., manuscript in preparation.

(45) Grätzel, M.; Moser, J.-E. *Electron Transfer in Chemistry*; Balzani, V., Gould, I., Eds.; Wiley-VCH: Weinheim, Germany, 2001.

(46) Tachibana, Y.; Haque, S. A.; Mercer, I. P.; Moser, J. E.; Klug, D. R.; Durrant, J. R. *J. Phys. Chem. B* **2001**, *105*, 7431 and references therein.

(47) Serpone, N.; Lawless, D.; Khairutdinov, R. *J. Phys. Chem.* **1995**, *99*, 16646.

(48) Li, G. H.; Yang, L.; Jin, Y. X.; Zhang, L. D. *Thin Solid Films* **2000**, *368*, 163.

(49) Reddy, K. M.; Reddy, C. V. G.; Manorama, S. V. *J. Solid State Chem.* **2001**, *158*, 180.

(50) Benkö, G.; Kallioinen, J.; Myllyperkiö, P.; Trif, F.; Korppi-Tommola, J. E. I.; Yartsev, A. P.; Sundström, V. *J. Phys. Chem. B* **2004**, *108*, 2862.

(51) Wallenberg, R.; Andersson, A.; Sanati, M. *Ultramicroscopy* **1990**, *34*, 33.

(52) Finnie, K. S.; Bartlett, J. R.; Woolfrey, J. L. *Langmuir* **1998**, *14*, 2744.

(53) Shklover, V.; Ovchinnikov, Y. E.; Braginsky, L. S.; Zakeeruddin, S. M.; Grätzel, M. *Chem. Mater.* **1998**, *10*, 2533.

(54) Asbury, J. B.; Anderson, N. A.; Hao, E.; Lian, T. *J. Phys. Chem. B* **2003**, *107*, 7376.